

APPLICATION OF VILENKIN'S ADDITIONAL THEOREM IN THE ANALYSIS OF SPHERICAL ANTENNAS AND PERIODIC STRUCTURES

Zvonimir Sipus and Sinisa Skokic

University of Zagreb, Faculty of Electrical Engineering and Computing
Unska 3, HR-10000 Zagreb, Croatia
E-mail: zvonimir.sipus@fer.hr, sinisa.skokic@fer.hr

ABSTRACT

This article demonstrates a novel approach to the mutual coupling calculation within the Moment Method (MoM) analysis of spherical arrays. By expressing the patch/dipole current in terms of two suitable potential-like auxiliary functions, it is possible to avoid the use of Euler's formulas for coordinate system rotation and the related lengthy integrations. Instead, the rotation in θ -direction can be done in closed form with the help of Vilenkin's additional theorem for associated Legendre functions. It is shown that the new approach results in significant acceleration of the analysis of both spherical antenna arrays and frequency selective surfaces. The algorithm is validated by comparing the results to the measurements performed on the developed laboratory model.

1. INTRODUCTION

Spherical antenna arrays present a natural choice if complete hemispherical coverage with nearly constant beam width is needed [1]. This makes them an optimal solution for satellite tracking applications, allowing simultaneous communication with multiple satellites from one base station. On the other hand, spherical periodic surfaces find their use as frequency selective radomes or sub-reflectors in reflector antenna systems.

In the analysis, spherical arrays are often approximated with a corresponding planar structure, and the spherical geometry is later accounted for by an appropriate coordinate and phase transformation. However, in many practical applications one cannot neglect the structure curvature. This is particularly important when accounting for the mutual coupling effects, since the magnitudes of mutual coupling coefficients depend strongly on the curvature. Mutual coupling can drastically change the embedded element pattern of each antenna element, and has to be rigorously included in the analysis procedure.

2. METHOD OF ANALYSIS

In this article, the rigorous analysis of arrays (of patches or printed dipoles), embedded in a multilayer spherical structure, is performed using the spectral-domain

approach. Both single patch and stacked-patch configurations are considered. The starting point for the analysis is the electric field integral equation (EFIE), which is solved using the moment method (MoM), while the elements of the MoM matrix are calculated in the spectral domain. The motivation for applying the spectral domain technique was to transform the three-dimensional problem into a spectrum of one-dimensional problems, which is much easier to solve [2], [3]. Since the problem is defined in the spherical coordinate system, this spectrum is obtained by applying the vector-Legendre transformation to the patch current [4], [3]. The Green's function of a general multilayer spherical structure is computed using the G1DMULT algorithm that calculates spectral domain Green's functions of general multilayer planar, circular cylindrical and spherical structures [3].

Direct implementation of the spectral-domain moment method is not possible for analyzing antennas mounted on a sphere of large radius because ratios of very large numbers need to be calculated. To find the numerically stable solution we have introduced normalized Legendre polynomials and an alternative definition of the vector-Legendre transformation. The vector-Legendre transformation is defined as (symmetrical definition, [5]):

$$\tilde{\mathbf{J}}(r, n, m) = \int_{-\pi}^{\pi} \int_0^{\pi} \frac{1}{\sqrt{2\pi S(n, m)}} \bar{\mathbf{L}}(n, m, \theta) \mathbf{J}(r, \theta, \phi) e^{-jm\phi} \sin\theta d\theta d\phi \quad (1a)$$

$$\mathbf{J}(r, \theta, \phi) = \sum_{m=-\infty}^{\infty} \sum_{n=|m|}^{\infty} \frac{1}{\sqrt{2\pi S(n, m)}} \bar{\mathbf{L}}(n, m, \theta) \tilde{\mathbf{J}}(r, n, m) e^{jm\phi} \quad (1b)$$

$$\bar{\mathbf{L}}(n, m, \theta) = \begin{bmatrix} P_n^{|m|}(\cos\theta) \sqrt{n(n+1)} & 0 & 0 \\ 0 & \frac{\partial P_n^{|m|}(\cos\theta)}{\partial\theta} & \frac{-jm P_n^{|m|}(\cos\theta)}{\sin\theta} \\ 0 & \frac{jm P_n^{|m|}(\cos\theta)}{\sin\theta} & \frac{\partial P_n^{|m|}(\cos\theta)}{\partial\theta} \end{bmatrix} \quad (1c)$$

$$S(n, m) = \frac{2n(n+1)(n+|m|)!}{(2n+1)(n-|m|)!} \quad (1d)$$

Here $P_n^{m|}(\cos\theta)$ denotes the associated Legendre function.

2.1. Mutual coupling calculation

When calculating the mutual coupling between the array elements, one needs to calculate the vector-Legendre transforms of basis and test functions with the domain on elements located at arbitrary positions on the sphere. In more details, the vector-Legendre transform of the i -th basis/test function defined on an arbitrarily positioned patch is:

$$\tilde{\mathbf{J}}_i(r, n, m) = \iint_{\text{patch}} \frac{1}{\sqrt{2\pi S(n, m)}} e^{jm\phi} \bar{\mathbf{L}}(n, m, \theta) \cdot \mathbf{J}_i(r, \theta', \phi') \sin\theta' d\theta' d\phi' \quad (2)$$

where θ and ϕ are coordinates in the global coordinate system, and θ' and ϕ' are coordinates in the local coordinate system (the local coordinate system is the one in which the center of the patch is at the sphere pole). Note that both matrix \mathbf{L} and basis functions \mathbf{J}_i are written with respect to the basis $(\hat{e}_\theta, \hat{e}_\phi, \hat{e}_r)$, which is the basis of the global coordinate system. In the standard approach, the current $\mathbf{J}(r, \theta', \phi')$ on the displaced element is translated to global coordinates by use of the Euler's formulas for coordinate system rotation [1]. Unfortunately, the vector Legendre transforms can no longer be computed in closed form, except for the centered element since only its basis/test functions have simple domain boundaries. All other terms need to be calculated numerically, resulting in lengthy integrations and slow analysis.

In the new approach, the analysis is made much more efficient by establishing the following relationship between the vector-Legendre transformation of the basis/test functions with the domain on the patch centered at the sphere pole ($\theta = 0$), and on the patch centered at $\theta = \alpha_n$, $\phi = \beta_n = 0$. As a first step, two functions \mathbf{A}^{J_i} and ψ^{J_i} are defined as

$$\mathbf{J}_i = \nabla \times \mathbf{A}^{J_i} + \nabla \cdot \psi^{J_i} \quad (3)$$

The chosen representation is similar to the representation of the electric field via vector and scalar potentials. Note that these formulas do not depend on coordinate system, i.e. they are valid in both global and local coordinate systems.

Noticing that the angular dependence in \mathbf{A}^{J_i} and ψ^{J_i} is present only in the term $e^{-jm\phi} P_n^{m|}(\cos\theta)$, we can relate

the representation of \mathbf{A}^{J_i} and ψ^{J_i} in different coordinate systems using the Vilenkin's addition theorem [6]:

$$e^{-jm\phi'} P_n^{m|}(\cos\theta') = j^m \left[\frac{(n+m)!}{(n-m)!} \right]^{1/2} \cdot \sum_{k=-n}^n j^{-k} \left[\frac{(n-k)!}{(n+k)!} \right]^{1/2} P_{m,k}^n(\cos\theta_{12}) P_n^{k|}(\cos\theta) e^{-jk\phi} \quad (4)$$

The function $P_{m,k}^n(\cos\theta_{12})$ is defined in [6] and θ_{12} is the rotation angle of the coordinate system. This gives us a simple and closed-form relationship which alleviates the need for numerical integration. As a result, the code based on the potential-like auxiliary functions is two orders of magnitude faster than a previously used code where the mutual coupling calculation was based on numerical integration.

2.2. Application to spherical FSS

A completely analogous procedure can also be applied to the analysis of spherical frequency selective surfaces (FSS). In this case, it is rather the excitation (plane wave) that has to be rotated, since it is only possible to obtain closed-form expressions for the vector-Legendre transform of the z-travelling plane wave, while the geometry of a FSS is best defined on the sphere equator.

The procedure is the following. We need to calculate the fields in the vicinity of the multilayer structure when the structure is excited by a plane wave. This can be done by using the spectral domain Green's function as, e.g., implemented in G1DMULT, provided we introduce current shells as sources generating the plane wave. In other words, we need to determine an equivalent current shell at a location above the multilayer structure which excites the given incident plane wave in the region of interest.

In spherical coordinate system, the incident plane wave can be expanded as

$$E(r, \theta, \phi) = \hat{x} E_0 e^{jkz} = -\frac{E_0}{kr} \sum_{m=\pm 1} \sum_{n=1}^{\infty} e^{jm\phi} \frac{j^{-n} (2n+1)}{n(n+1)} \cdot \left\{ \hat{\theta} \left[\hat{J}_n(kr) \frac{P_n^1(\cos\theta)}{\sin\theta} + j \hat{J}'_n(kr) \frac{\partial P_n^{1|}(\cos\theta)}{\partial\theta} \right] + \hat{\phi} jm \left[\hat{J}_n(kr) \frac{\partial P_n^{1|}(\cos\theta)}{\partial\theta} + j \hat{J}'_n(kr) \frac{P_n^1(\cos\theta)}{\sin\theta} \right] \right\} \quad (5)$$

The amplitude of the equivalent current shell of one spectral component is equal (we need to specify two components of the equivalent magnetic current shell,

and two components of the equivalent electric current shell; these values are the input variables to the G1DMULT routine):

$$\begin{aligned}\tilde{\mathbf{M}}_{eq}(r_{eq}, n, m) &= \frac{E_0}{kr} j^{-n} 2\sqrt{\pi(2n+1)} \delta(|m|-1) \\ &\quad \cdot \left\{ \hat{\theta} \cdot (jm \hat{J}_n(kr_{eq})) + \hat{\phi} \cdot (-j \hat{J}'_n(kr_{eq})) \right\} \\ \tilde{\mathbf{J}}_{eq}(r_{eq}, n, m) &= \frac{E_0}{\eta kr} j^{-n} 2\sqrt{\pi(2n+1)} \delta(|m|-1) \\ &\quad \cdot \left\{ \hat{\theta} \cdot (-\hat{J}_n(kr_{eq})) + \hat{\phi} \cdot (m \hat{J}'_n(kr_{eq})) \right\}\end{aligned}\quad (6)$$

These equations are valid only for a plane wave traveling in the (negative) z direction. If one wants to consider a plane wave with an arbitrary angle of incidence (i.e. $\theta^{inc} \neq 0$), one needs to find the representation of the equivalent currents in the rotated coordinate system. Following the described procedure (eqs. 3-4), one can find that the needed potential-like auxiliary functions are (e.g. for equivalent magnetic current):

$$\begin{aligned}A_r^{M_{eq}}(r_{eq}, \theta, \phi) &= \sum_{k=-\infty}^{\infty} \sum_{n=|k|}^{\infty} P_n^{|k|}(\cos \theta) e^{jk\phi} \\ &\quad \cdot \left\{ -\sum_{m=\pm 1} (-j)^{1-|k|} \sqrt{\frac{(n+1)!}{(n-1)!}} \sqrt{\frac{(n-|k|)!}{(n+|k|)!}} P_{1, \text{sign}(m) \cdot k}^n(\cos \theta_{12}) \right. \\ &\quad \cdot \left. \frac{E_0}{kr} \frac{j^{-n}(2n+1)}{n(n+1)} \cdot (-j \hat{J}'_n(kr_{eq})) \right\} \\ \psi^{M_{eq}}(r_{eq}, \theta, \phi) &= \sum_{k=-\infty}^{\infty} \sum_{n=|k|}^{\infty} P_n^{|k|}(\cos \theta) e^{jk\phi} \\ &\quad \cdot \left\{ \sum_{m=\pm 1} (-j)^{1-|k|} \sqrt{\frac{(n+1)!}{(n-1)!}} \sqrt{\frac{(n-|k|)!}{(n+|k|)!}} P_{1, \text{sign}(m) \cdot k}^n(\cos \theta_{12}) \right. \\ &\quad \cdot \left. \frac{E_0}{kr} \frac{j^{-n}(2n+1)}{n(n+1)} \cdot (jm \hat{J}_n(kr_{eq})) \right\}\end{aligned}\quad (7)$$

3. RESULTS

We have implemented the described enhancements in the program and tested it both on a FSS configuration and a patch antenna array configuration. The results were verified with a commercially available software and with measurements where possible.

3.1. Spherical FSS

The simulated test cases all included a FSS on a spherical shell of radius $r = 19.22$ cm in free space. We consider a 250 element array (5 by 50) with θ -directed dipoles. The dipoles are 4 cm long and the distance

between the neighbouring element centers is 0.5 cm and 4.33 cm in ϕ - and θ -direction, respectively. The incident electric plane wave is y -polarized and travelling in the $-x$ direction, as shown in Fig.1. The frequency is 2 GHz unless explicitly noted.

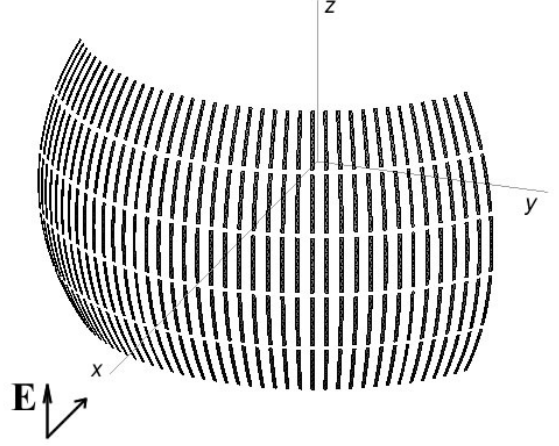


Figure 1. 5 x 50 spherical array (FSS)

The calculated results were compared to those obtained with a commercially available solver (FEKO™). Even though both programs are MoM-based, this verification is still valid because the approach to the problem is quite different. To be more specific, while in our code we treat the problem immediately in spectral domain with entire-domain basis functions in spherical coordinates, a conventional solver such as FEKO™ applies a more general procedure that meshes the object under consideration into triangular and rectangular subsections and approximates the curved surface with a locally planar one.

The comparison of the calculated bistatic Radar Cross Section by both methods is shown in Fig.2 and Fig.3. One can see that the two results agree almost perfectly in both azimuthal and elevation plane.

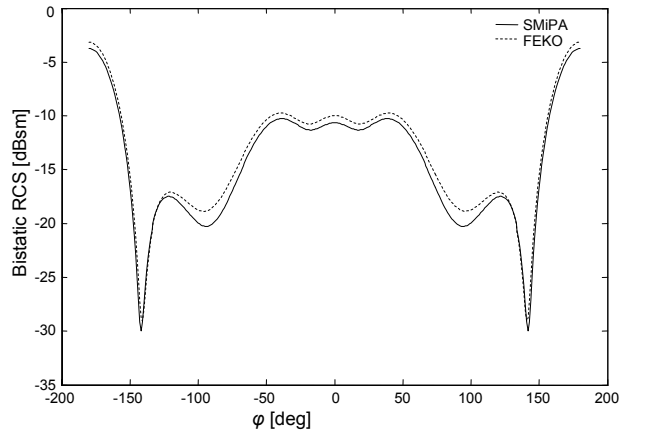


Figure 2. Bistatic RCS of a 5 x 50 spherical gangbuster array in azimuthal plane ($\theta=90^\circ$), for broadside wave illumination.

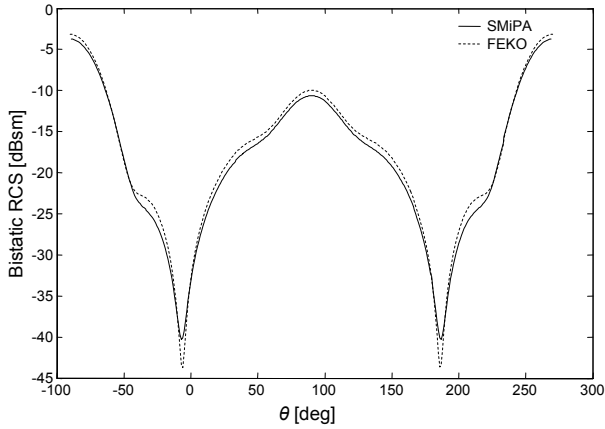


Figure 3. Bistatic RCS of a 5 x 50 spherical gangbuster array in elevation plane ($\varphi=0^\circ$), for broadside wave illumination.

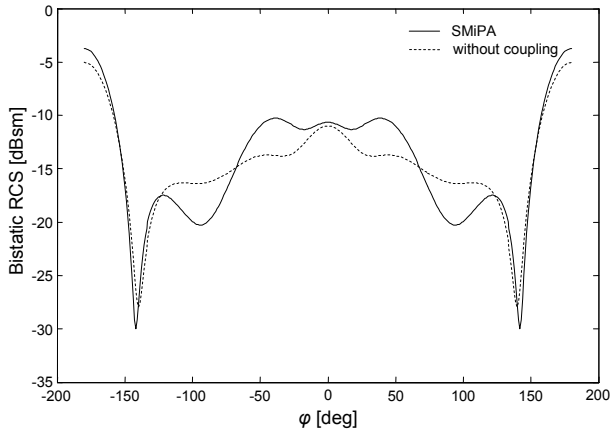


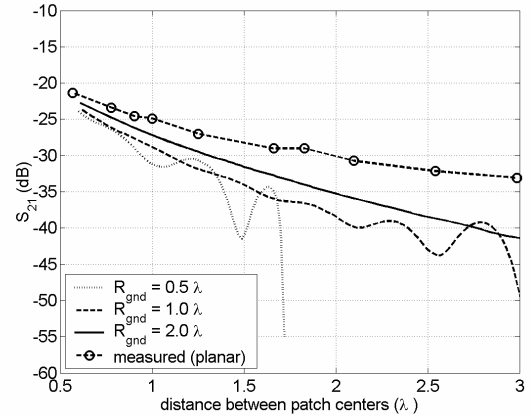
Figure 4. Comparison of the bistatic RCS of a 5 x 50 array in the azimuthal plane ($\theta=90^\circ$), with and without mutual coupling taken into account.

The importance of the full-wave approach to the FSS analysis is illustrated in Fig.4. The azimuthal plane RCS pattern of a 5x50 array of θ -dipoles is confronted to the case where the amplitudes of dipole currents have all been taken equal and the phase distribution follows the phase of the incident plane wave on the surface of the sphere (i.e. neglecting mutual coupling). One can notice differences up to 5 dB at some angles, which is rather significant.

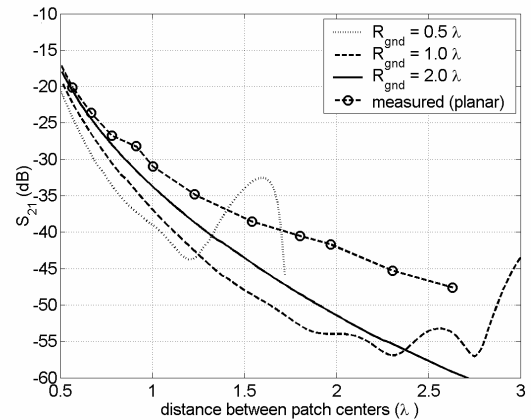
3.2. Circular patch antennas on spherical structures

In the second test configuration, we investigated the influence of the sphere radius on mutual coupling level (Fig. 5). We considered an array of two circular patch antennas. The diameter of the patches is 1.86 cm and they are printed on a grounded dielectric layer with $\epsilon_r = 12.5$ and $h_l = 0.16$ cm. The position of the feed point is 0.794 cm relative to the patch center. The magnitude of the S_{21} parameter, both in E - and H -plane, is shown as a

function of spacing between patch edges. The coupling level is compared to the measured results of the equivalent planar case [7]. It can be seen that the coupling is weaker in the spherical case than in the planar one. For smaller structure radii mutual coupling starts to be oscillatory due to interference of forward and backward propagating waves around the sphere.



(a)

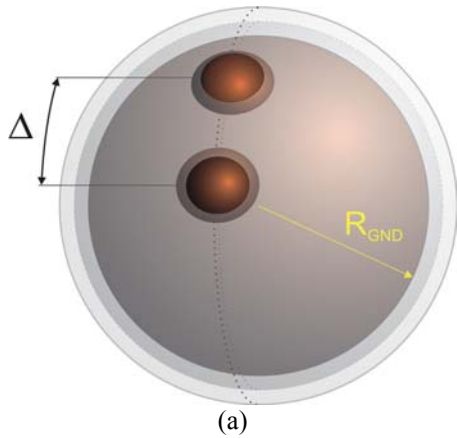


(b)

Figure 5. Calculated magnitude of S_{21} parameter of a two-patch array as a function of spacing between patch centers; (a) E -plane coupling, (b) H -plane coupling.

In order to validate the program for stacked-patch configurations, a laboratory model was developed where it is simple to measure different array configurations (Fig. 6). The model was built from a copper sphere of radius $a = 18.5$ cm on which patches were mounted at different positions. The mounting of patches at arbitrary positions is very simple: one just needs to place an SMA connector at the desired position on the grounded shell. We have built an arrays of two stacked-patches coupled in E -plane (see Fig. 6). The thickness of both layers is $h_1 = h_2 = 5.2$ mm. The diameters of the lower and upper patches are 6.2 cm and 5.45 cm, respectively. The lower patch is excited with a coaxial transmission line, and the excitation position is

2.0 cm relative to the patch center. Small Styrofoam cubes ($\epsilon_r \approx 1.0$) are used as spacers between patches and the grounded shell. Note that the patches are made from a sphere of appropriate radius since it is important that patches follow the spherical structure.



(b)

Figure 6. Sketch (a) and photo (b) of the developed laboratory model.

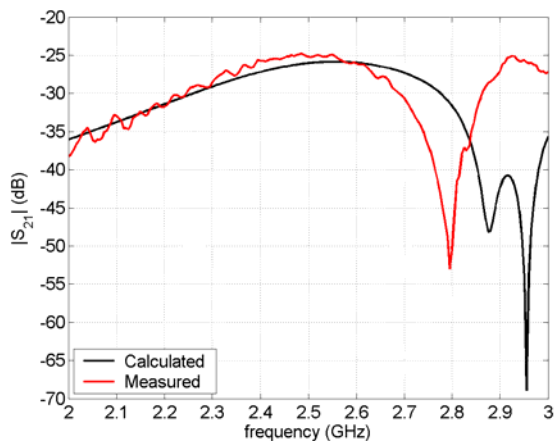


Figure 7. Calculated and measured magnitude of S_{21} parameter of a two-patch array of circular stacked-patches.

The comparison of measured and calculated mutual coupling level is shown in Fig. 7. The agreement between results is good, except for the small frequency shift.

CONCLUSION

A new technique for calculating the mutual coupling in the Moment Method (MoM) analysis of spherical arrays has been developed. The technique consists of defining two potential-like auxiliary functions which contain the information about the coordinates only in respective arguments of a product of Legendre and exponential functions. This term can then be transformed from one coordinate system to another very simply, by use of the Vilenkin's additional theorem.

The new technique has been implemented in the previously developed MoM code for the analysis of spherical arrays and frequency selective surfaces. Compared to the standard algorithm, two orders of magnitude shorter simulation times were achieved with the new technique. A laboratory model was also built to verify the correctness of the obtained results.

REFERENCES

1. D.L. Sengupta, T. M. Smith, R. W. Larson, *Radiation Characteristics of Spherical Array of Circularly Polarized Elements*, IEEE Trans. on Antennas and Propagation., Vol. 16, pp. 2-7, 1968.
2. R. F. Harrington, *Time-harmonic electro-magnetic waves*, McGraw-Hill, 1961.
3. Z. Sipus, P.-S. Kildal, R. Leijon, M. Johansson, *An algorithm for calculating Green's functions for planar, circular cylindrical and spherical multilayer substrates*, Applied Computational Electromagnetics Society Journal, Vol. 13, pp. 243-254, 1998.
4. W. Y. Tam, K. M. Luk, *Resonances in spherical-circular microstrip structures of cylindrical-rectangular and wraparound microstrip antennas*, IEEE Trans. Microwave Theory Tech., Vol. 39, pp. 700-704, 1991.
5. Z. Sipus, N. Burum, S. Skokic, P.-S. Kildal, *Analysis of spherical arrays of microstrip antennas using moment method in spectral domain*, accepted for publication in IEE Proc. – Microw. Antennas Propag.
6. N. Ja. Vilenkin, *Special Functions and the Theory of Group Representation*, American Mathematical Society, Providence, 1968.
7. M.D. Deshpande, M.C. Bailey, *Analysis of finite arrays of circular microstrip patches*, IEEE Trans. on Antennas and Propagat., Vol. 37, pp. 1355-1360, 1989.